

v-SNARE Actions during Ca^{2+} -Triggered Exocytosis

Jaideep Kesavan,^{1,2} Maria Borisovska,^{1,2} and Dieter Bruns^{1,*}

¹University of Saarland, Institute for Physiology, Kirrberger Street 8, D-66424 Homburg/Saar, Germany

²These authors contributed equally to this work.

*Correspondence: dieter.bruns@uniklinik-saarland.de

DOI 10.1016/j.cell.2007.09.025

SUMMARY

Assembly of SNARE proteins between opposing membranes mediates fusion of synthetic liposomes, but it is unknown whether SNAREs act during exocytosis at the moment of Ca^{2+} increase, providing the molecular force for fusion of secretory vesicles. Here, we show that execution of pre- and postfusional steps during chromaffin granule exocytosis depends crucially on a short molecular distance between the complex-forming SNARE motif and the transmembrane anchor of the vesicular SNARE protein synaptobrevin II. Extending the juxtamembrane region of synaptobrevin by insertion of flexible “linkers” reduces priming of granules, delays initiation of exocytosis upon stepwise elevation of intracellular calcium, attenuates fluctuations of early fusion pores, and slows rapid expansion of the pore in a linker-length dependent fashion. These observations provide evidence that v-SNARE proteins drive Ca^{2+} -triggered membrane fusion at millisecond time scale and support a model wherein continuous molecular pulling by SNAREs guides the vesicle throughout the consecutive stages of exocytosis.

INTRODUCTION

To accomplish fusion, membranes must overcome large energy barriers created by local dehydration of polar phospholipid headgroups and membrane deformation. Surmounting these barriers requires the action of proteins with special capabilities to lower the energy costs. The important role of SNARE proteins has been shown in various membrane trafficking pathways (Jackson and Chapman, 2006; Jahn and Scheller, 2006). Reconstitution experiments in liposomes suggested that heterotrimeric SNARE complexes are able to promote fusion, albeit at a slow time scale (Weber et al., 1998; Nickel et al., 1999; Pobbati et al., 2006). In general, at least one SNARE protein is anchored in the vesicular membrane (v-SNARE), whereas another SNARE is anchored in the target membrane

(t-SNARE). By binding one another, SNAREs may force these membranes into close proximity, resulting in hemifusion (mixing of the outer lipid monolayers) and ultimately leading to aqueous content mixing as observed for in vitro fusion (Giraud et al., 2005; Reese et al., 2005; Xu et al., 2005). Yet, the behavior of reconstituted fusion systems varies widely across laboratories and recent data have challenged the idea that SNARE assembly triggers fusion between synthetic membranes (Bowen et al., 2004; Dennon et al., 2006). Even more unclear is whether this scenario holds for rapid Ca^{2+} -triggered exocytosis and if so, at which stages the exocytotic process depends on mechanical strain between the complex-forming SNARE domain and the transmembrane domain (TMD). To address these issues in vivo, we expressed synaptobrevin II (sybII) mutant proteins carrying an extended juxtamembrane region in mouse chromaffin cells that are genetically deficient for sybII and cellubrevin (double-knockout cells, dko) and nearly devoid of secretion (Borisovska et al., 2005). In following this strategy, we intended to increase the physical distance between the SNARE domain and the TMD and studied Ca^{2+} -dependent exocytosis mediated by v-SNARE mutants in a gain-of-function approach. By using a combination of high-resolution membrane capacitance measurements, amperometry and photolytic “uncaging” of intracellular calcium, we track v-SNARE function at the millisecond time scale from pre- to postfusional stages that either do not exist or cannot be detected in in vitro assays. Our results indicate multiple v-SNARE actions from granule priming to membrane merger and suggest that persistent molecular straining by SNAREs guides the vesicle on the way toward complete fusion. They further provide experimental support that v-SNAREs exert force on membranes to initiate fusion at the moment of the intracellular Ca^{2+} increase, meeting the speed requirement of regulated exocytosis.

RESULTS

Priming and Fast Stimulus-Secretion Coupling Demand a Tight Molecular Link between SNARE Domain and Transmembrane Anchor of SybII

The insertion of a flexible, 11 amino acid linker in the juxtamembrane region of sybII only moderately diminished fusion (<20%) between artificial liposomes (McNew

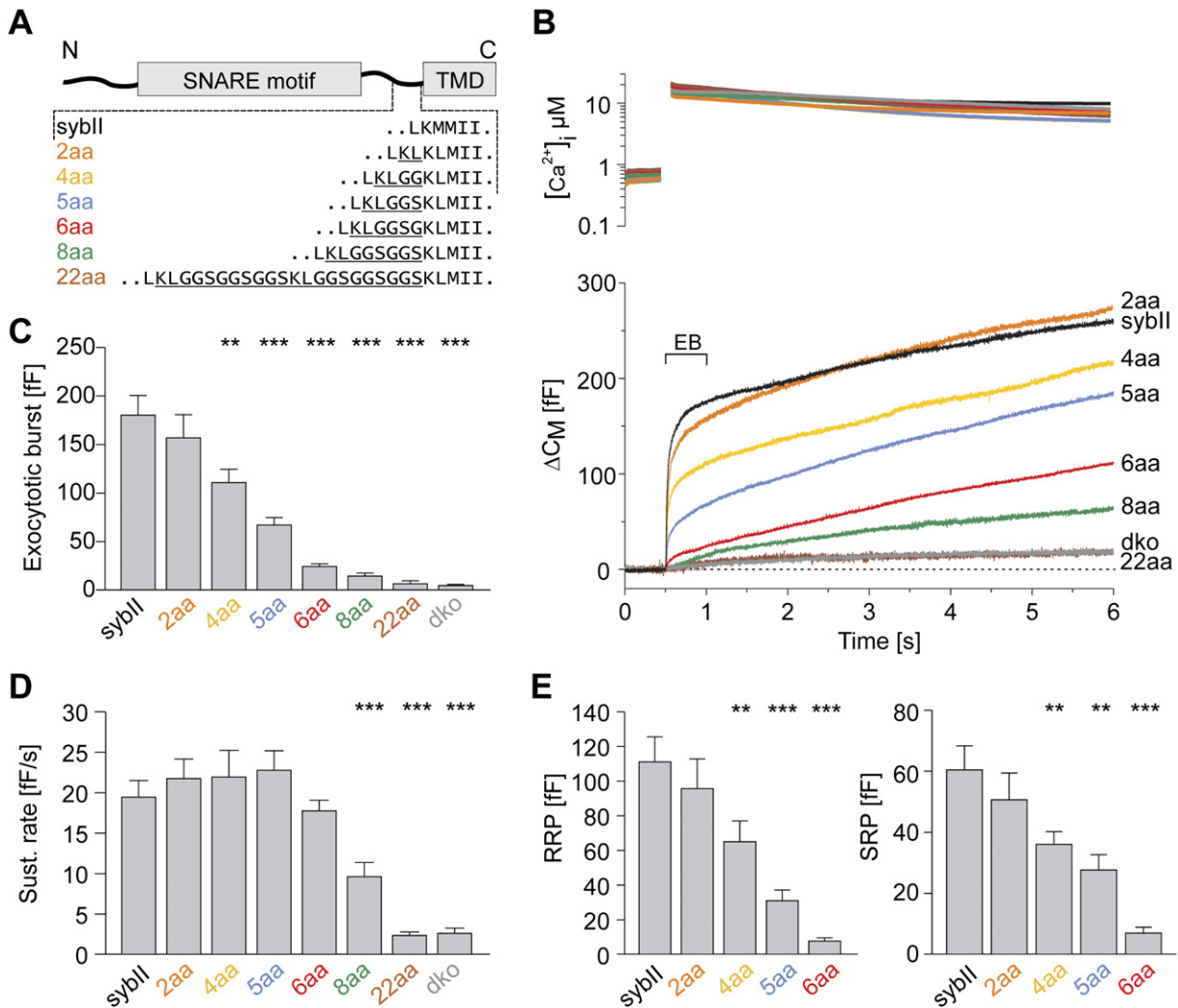


Figure 1. Extending the Juxtamembrane Region of SybII Gradually Reduces the Flash-Evoked Capacitance Response

(A) Schematic view of sybII domains. SNARE motif and transmembrane domain (TMD) are boxed. Underlined amino acid sequences show the insertions intended to increase the physical distance and/or flexibility between SNARE domain and TMD.

(B) Average flash-evoked $[Ca^{2+}]_i$ increases (upper panel) and corresponding capacitance responses (lower panel) of dko cells expressing sybII ($n = 25$) or mutated sybII variants. Amino acid insertions of increasing length (2 aa, $n = 13$; 4 aa, $n = 23$; 5 aa, $n = 30$; 6 aa, $n = 41$) gradually decrease the exocytotic burst (EB). Longer insertions (e.g., 8 aa, $n = 18$) also attenuate the sustained phase of secretion. The 22 aa mutant ($n = 10$) fails to support any exocytosis when compared with dko ($n = 17$). Flash, $t = 0.5$ s.

(C and D) Linker-length dependence of the exocytotic burst size (EB, measured 0.5 s after flash) and the sustained phase of secretion.

(E) Both, RRP (left panel) as well as SRP (right panel) gradually decrease with increasing linker length. ** $p < 0.01$, *** $p < 0.001$ versus sybII, one-way analysis of variance.

et al., 1999). Surprisingly, expression of a similar mutant protein (8 amino acid insertion, 8 aa) in dko cells fails to restore the initial capacitance increase (also referred to as exocytotic burst component, EB) that is seen with the wild-type protein in response to the step-wise Ca^{2+} stimulus (Figures 1A and 1B). Decreasing the length of the insertion to 6, 5, 4, and 2 amino acids (6 aa, 5 aa, 4 aa, and 2 aa) progressively increases the ability of the mutant protein to rescue the capacitance signal (Figures 1B and 1C). With the 2 aa insertion, a nearly complete restoration of the flash-evoked response has been reached. For

further analyses, the capacitance response from each cell was approximated by the sum of two exponentials and a linear rate to estimate the size of the fast (readily releasable pool, RRP) and the slow (slowly releasable pool, SRP) phase of release within the exocytotic burst as well as the subsequent sustained release phase (Experimental Procedures). Both components of the exocytotic burst, RRP and SRP, are similarly affected by the amino acid insertions (Figure 1E), indicating that linker mutants interfere with the establishment or maintenance of these release-ready states. Thus, the exocytotic burst, a measure of

the number of primed granules (Rettig and Neher, 2002), exhibits a stringent length requirement of the juxtamembrane region. In contrast, the subsequent sustained release phase decreases significantly only with insertions longer than 6 aa and is fully abolished with further extension of the juxtamembrane region (e.g., 22 aa, Figure 1D). The latter phase of release may either reflect the generation of newly primed vesicles that undergo fusion as long as calcium is high (Voets et al., 1999) or, analogous to neuronal secretion, represent a slow asynchronous form of exocytosis devoid of molecular factors, like complexin, which is required for exocytosis synchronization (Reim et al., 2001). In any case, the initial (synchronous) and subsequent (asynchronous) release phase similarly depends on v-SNARE proteins, as illustrated by their strong block in dko cells. To investigate whether linker mutants assemble into SNARE complexes *in vivo*, we studied the effect of the 22 aa linker on exocytosis of wild-type cells. Overexpression of the mutant protein reduces exocytosis by more than 60% compared with sybII expression (see Figure S1 in the Supplemental Data available with this article online). This demonstrates that the 22 aa mutant is able to compete with endogenous sybII and to bind its cognate SNARE partners, but forms complexes that are nonproductive for fusion, as judged from its inability to restore secretion in dko cells. The remaining exocytosis in wild-type cells expressing the 22 aa mutant is likely mediated by endogenous sybII, emphasizing the importance of a genetic “null” background for the analysis of v-SNARE function. Taken together, a short molecular distance or high strain between the complex-forming domain and the TMD of the v-SNARE protein is needed for release readiness of chromaffin granules, whereas longer extensions of the juxtamembrane region abolish their fusion competence. The latter observation is compatible with a recent study, showing that expression of sybII mutants with similarly long amino acid insertions (e.g., 24 aa) in sybII-deficient neurons fails to restore destaining of styryl dye labeled synapses upon stimulation with high-potassium application (Deak et al., 2006).

A key question toward the understanding of SNARE function in exocytosis is whether these proteins act at the moment of the Ca^{2+} rise. To address this issue, we analyzed how lengthening of sybII's juxtamembrane region affects exocytosis timing. Averaged sybII and mutant responses with a sizable exocytotic burst (>20 fF) are shown in Figure 2A and displayed on an extended time scale (first 40 ms after the flash) in Figure 2B. Increasing the linker length causes a systematic increase in the time lag between UV-flash and onset of the capacitance signals triggered by nearly identical postflash $[\text{Ca}^{2+}]_i$ (Figure 2D). Scaling of the capacitance signals to the exocytotic burst size measured with sybII (0.5 s after the flash) shows that the delayed onset of mutant secretion is followed by a capacitance increase with unchanged kinetics (Figure 2C). Apparently, mutant secretion is shifted to later times after the flash, suggesting that readily releasable vesicles equipped with a mutant protein fuse with the plasma

membrane upon Ca^{2+} elevation after an additional time lag. Kinetic rates of the exocytotic burst components (reciprocal of the exponential time constants t_{RRP} and t_{SRP}) as well as the latency between UV-flash and start of secretion were estimated by exponential fitting of the individual cellular responses. These results confirm the finding that amino acid insertions confer a significant and graded delay in exocytosis (sybII: 4.1 ± 0.5 ms; 4 aa: 5.8 ± 0.5 ms; 5 aa: 8.4 ± 0.7 ms; 6 aa: 14.0 ± 1.3 ms, Figure 2E). In good agreement with the averaged recordings, the rates of exocytosis from RRP and SRP resemble closely those of the sybII-mediated signals (Figures 2F and 2G; $p > 0.7$).

For chromaffin cells, the exocytotic delay is largely determined by the kinetics of Ca^{2+} binding to synaptotagmin I serving as the primary Ca^{2+} sensor for exocytosis (Voets et al., 2001; Nagy et al., 2006). As shown in Figure 2H, the delay of sybII signals strongly decreases with increasing $[\text{Ca}^{2+}]_i$. For 6 aa mutant responses, however, exocytotic delays are prolonged over the entire range of investigated Ca^{2+} concentrations. In contrast, the Ca^{2+} -dependent rates of exocytosis from RRP are similar to those of sybII responses (Figures 2H and 2I). Notably, adding a constant time lag of 9 msec to the measured sybII delays reveals a reasonable overlap with the distribution of mutant delays (Figure 2H). Even at high $[\text{Ca}^{2+}]_i$, in the range of 50–70 μM , 6 aa mutant exocytosis maintains a clear time lag of 6–10 msec compared with sybII. These findings strongly suggest that linker mutations prolong the latency between stimulus and onset of exocytosis in a Ca^{2+} -independent fashion. To substantiate this observation, we determined the Ca^{2+} threshold of sybII and mutant secretion using a ramp-like calcium stimulus (Sorensen et al., 2002). In these experiments, intracellular calcium is slowly “uncaged” by alternating illumination with 340 and 380 nm using the monochromator. The comparison of the capacitance signals in response to the rise of $[\text{Ca}^{2+}]_i$ reveals similar Ca^{2+} thresholds for sybII- and 6 aa-mediated secretion (Figure 3). Taken together, these results show that amino acid insertions immediately preceding the TMD cause an additional delay in stimulus-secretion coupling without altering the apparent Ca^{2+} sensitivity of exocytosis. The most straightforward interpretation of these observations is that at the moment of the Ca^{2+} rise, SNARE proteins exert force on membranes to initiate fusion, whereas linker insertions partially dissipate this force leading to a delayed reaction. In contrast, expression of a v-SNARE variant, which carries two helix-breaking proline residues (PP mutant) instead of a flexible linker, enables a nearly complete rescue of the capacitance response with no changes in the exocytotic delay (Figure S1). Thus, distance and/or flexibility rather than helical continuity between the SNARE domain and the TMD (Sutton et al., 1998) are responsible for the linker-length dependent effects on pool size and exocytosis onset. Furthermore, v-SNARE mutants do not differ from sybII protein regarding the level or pattern of protein expression in dko cells, suggesting that extension of the protein's juxtamembrane region causes the observed phenotypes (Figure S2).

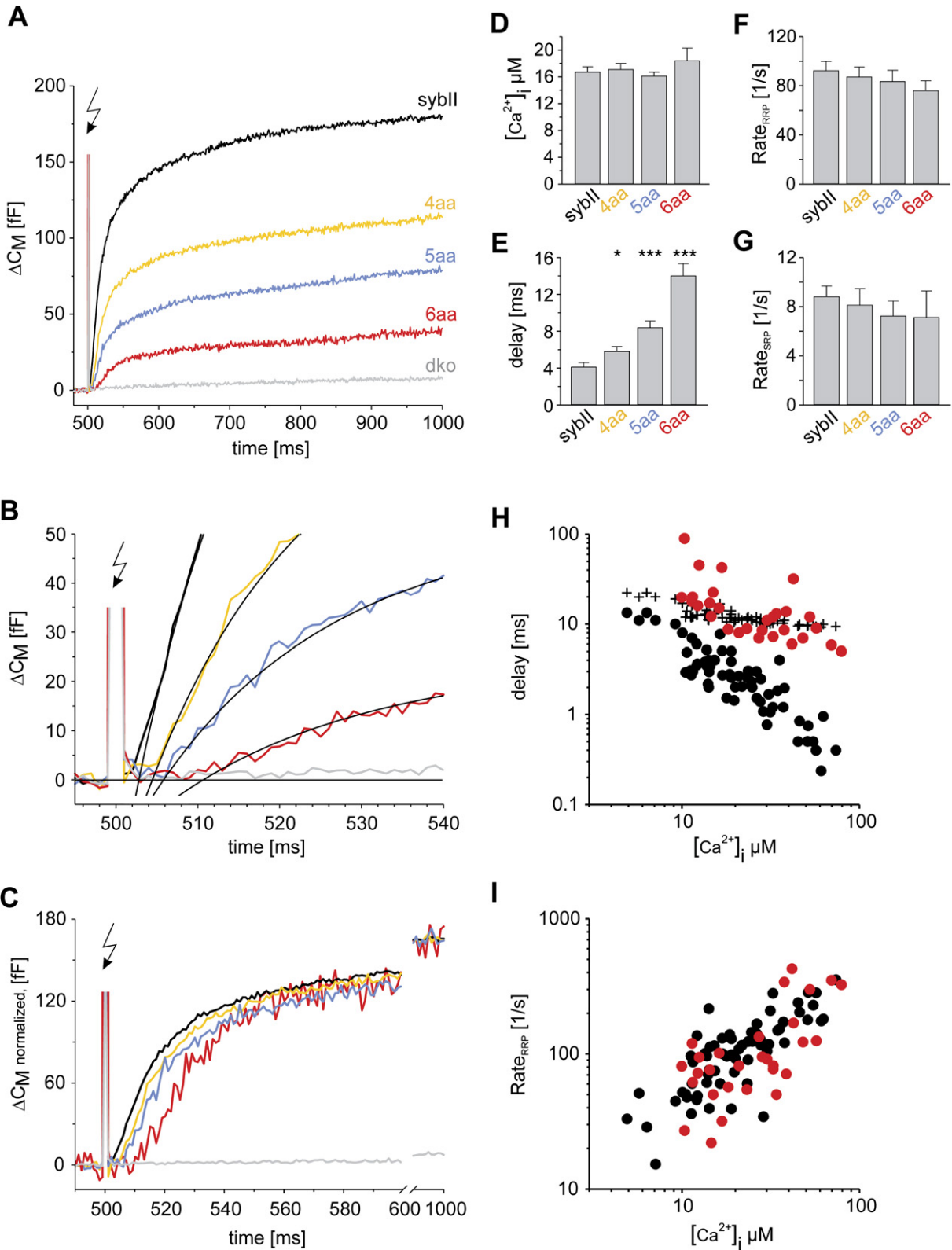


Figure 2. Extension of Syb1's Juxtamembrane Region Delays Granule Exocytosis without Changing the Ca^{2+} Dependence of Secretion

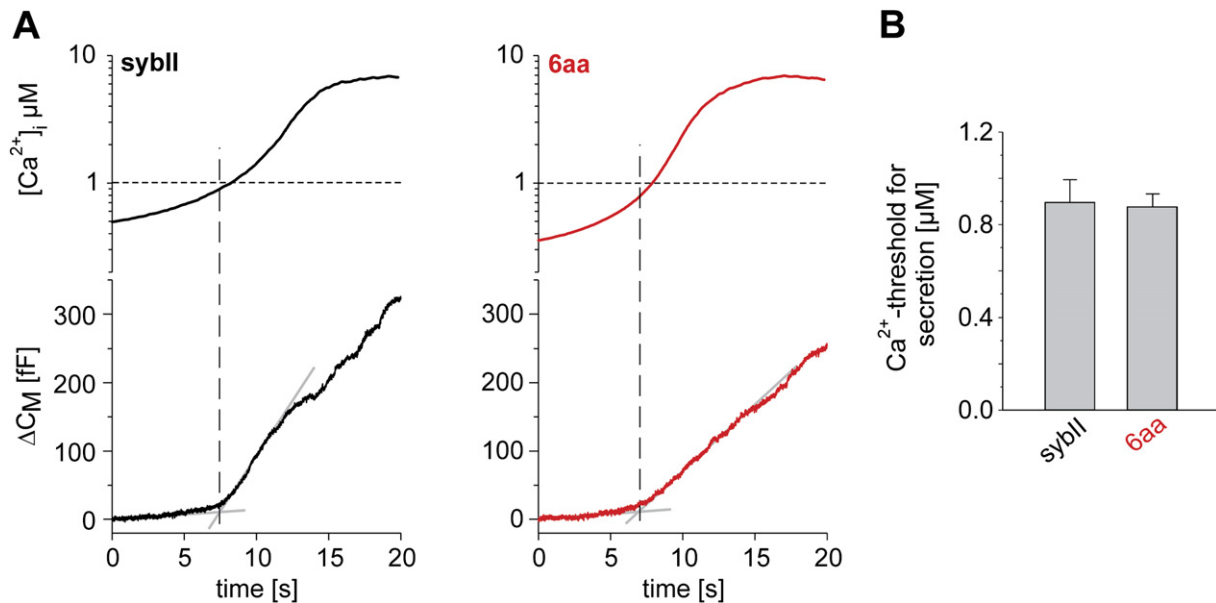


Figure 3. Linker Mutations Do Not Affect the Apparent Ca^{2+} Threshold of Secretion

(A) Exemplary recordings of the capacitance signals (lower panels) of dko cells expressing sybll (left) or 6 aa mutant (right) in response to a slow, ramp-like rise in $[\text{Ca}^{2+}]_i$ (upper panels). The point of intersection between two linear regressions (gray lines) approximating the baseline (1–3 s) and the steep rise of the capacitance response defines the threshold for secretion (dashed line).

(B) The Ca^{2+} thresholds for secretion of sybll and 6 aa expressing cells are indistinguishable (sybll, $n = 20$; 6 aa, $n = 26$, $p > 0.8$, Students t test).

Postfusional Control of Quantal Discharge by Sybll

Encouraged by the above findings, we studied the functional impact of linker mutations at the resolution level of single vesicle release using amperometry. In these experiments, exocytosis was stimulated by intracellular perfusion with high Ca^{2+} -containing solution (19 μM free calcium) and monitored simultaneously with membrane capacitance measurements and carbon fiber amperometry. This allowed us to gather a large number of exocytotic events that could be resolved as well-separated amperometric spikes. Upon the start of intracellular Ca^{2+} perfusion, sybll expressing cells respond with a strong increase in the frequency of amperometric signals as well as in membrane capacitance (Figure 4A). In comparison, linker mutants carrying long amino acid insertions (e.g., 14 aa)

promote a reduced secretory response to such a Ca^{2+} stimulus. Both assays for secretion, membrane capacitance and amperometry, reveal a linker-length dependent attenuation in exocytotic activity and a complete loss of secretion with the 22 aa insertion (Figure 4C). These results support several important conclusions. The close correspondence between the two independent measurements ($r = 0.99$, $p < 0.001$) shows that the observed changes in the capacitance signal are due to alterations in granule exocytosis. Furthermore, they demonstrate that Ca^{2+} -triggered asynchronous exocytosis, measured here as perfusion-induced capacitance increase, is less sensitive to lengthening of the juxtamembrane region than the exocytotic burst component in the flash experiment (Figure 4E). This may suggest that the two forms of

(A) Ca^{2+} -triggered capacitance signals during the first 500 ms after the flash. Data are averaged from dko cells expressing sybll ($n = 25$) or its mutated variants (4 aa, $n = 22$; 5 aa, $n = 19$; 6 aa, $n = 14$) with an exocytotic burst size > 20 fF in response to average postflash $[\text{Ca}^{2+}]_i$, ranging from 16.1 to 18.4 μM as shown in (D). Secretion from dko cells ($n = 17$) in response to similar $[\text{Ca}^{2+}]_i$ (15.0 \pm 1.4 μM) is nearly abolished ($< 7\%$ of sybll-mediated secretion at 0.5 s after the flash). Arrow indicates flash artifact.

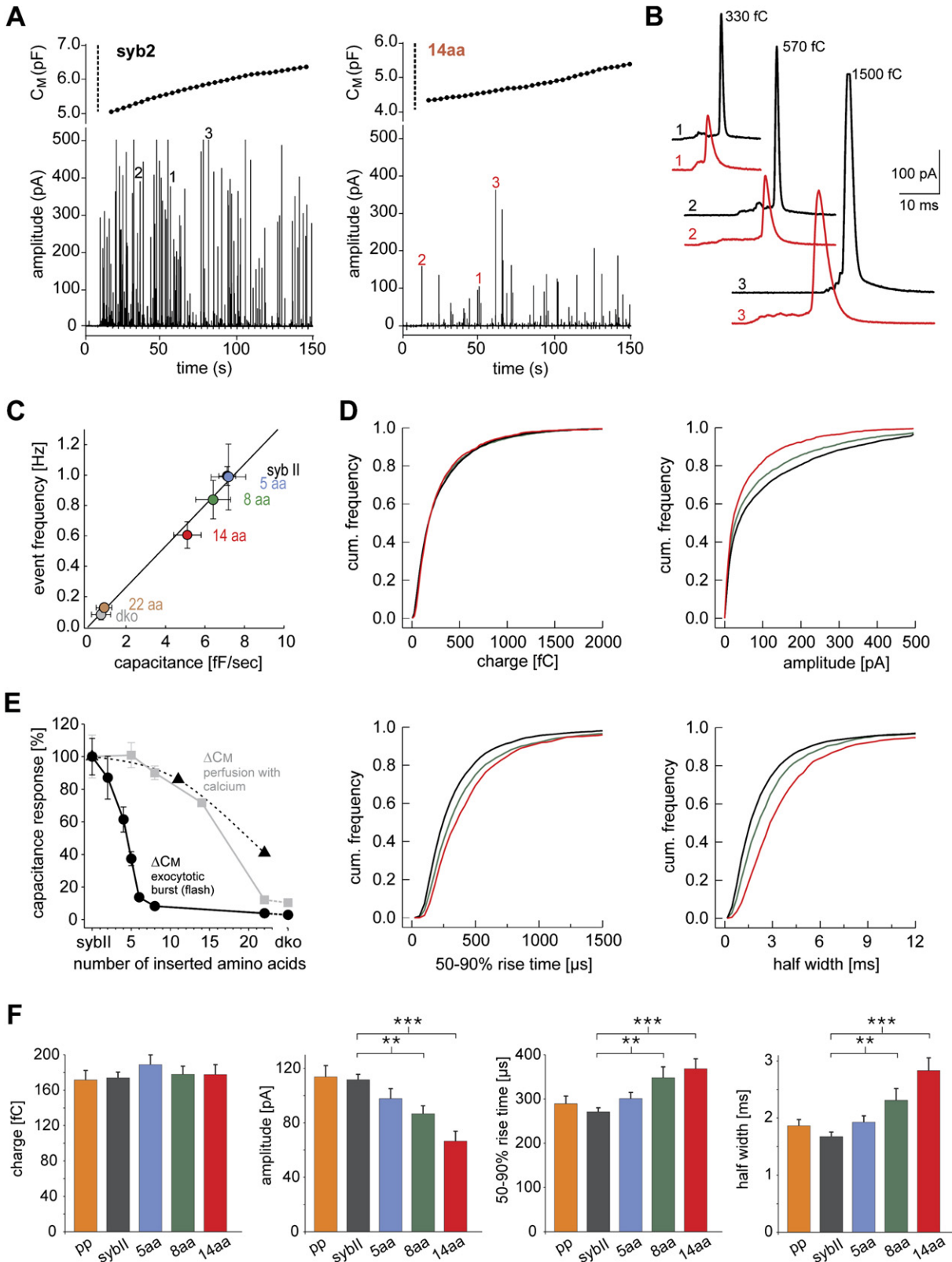
(B) Extended scaling of capacitance responses shown in (A) during the first 40 ms after flash. Compared with sybll (black), insertion of 4 (yellow), 5 (blue), or 6 (red) amino acids progressively delays the onset of secretion defined as intersection point between the back extrapolated fast exponential (black lines) and the baseline. (C) The delayed onset of mutant secretion is followed by a capacitance increase with rates similar to those of sybll. Capacitance signals (as shown in A) are normalized to the exocytotic burst size of the sybll response (0.5 s after the flash) after subtraction of the sustained release component (see Figure 1D) and of the background signal measured in dko cells.

(D) The average postflash $[\text{Ca}^{2+}]_i$ values for the responses shown in (A) are nearly identical.

(E) The mean exocytotic delay determined from fitting individual cellular responses increases significantly with linker extension. * $p < 0.05$, *** $p < 0.001$, one-way analysis of variance versus sybll.

(F and G) Mean rates of RRP and SRP exocytosis measured for sybll and linker mutants.

(H and I) Stimulus-secretion coupling of sybll (black circles, $n = 64$) and 6 aa mutant (red circles, $n = 30$) exocytosis as a function of flash-induced $[\text{Ca}^{2+}]_i$. The delayed onset of mutant secretion persists over the entire range of calcium concentrations tested. Adding 9 ms to each sybll delay (black crosses) creates a reasonable overlap with the distribution of mutant delays. The rates of RRP exocytosis measured for sybll and 6 aa are similar.



v-SNARE-dependent exocytosis, synchronous and asynchronous exocytosis, are molecularly different, as will be discussed below. In addition, the delayed onset of secretion seen with short insertions (Figure 2) together with the strong block of exocytosis by longer insertions (Figure 4E) indicates that increasing the physical distance between the SNARE domain and the TMD progressively inhibits fusion. Interestingly, amperometric signals mediated by longer linker mutants differ not only in frequency, but also show clear changes in the kinetics of transmitter discharge from single vesicles, compatible with the phenotype of a fusion mutant. As depicted for pairs of exemplary events with similar charge in Figure 4B, signals recorded upon expression of the 14 aa mutant protein (red) are characterized by significantly lower amplitudes and slower discharge kinetics when compared with sybII-mediated events (black). A comparison of the frequency distributions of the parameters as well as of the cell-weighted averages confirms the strong and significant reduction in event amplitude measured for the 8 aa mutant that is even further decreased for the 14 aa mutant (Figures 4D and 4F). In close correlation, rise time and half width of the mutant spikes are gradually prolonged without changing the event charge. For the PP mutant, no changes in the event properties are found. The preserved quantal size as well as the close correlation between membrane capacitance measurement and amperometric event frequency counter the possibility that alterations of the release time course are due to premature closure of the fusion pore, but instead suggest slower fusion pore expansion. Thus, tight coupling between the SNARE domain and the TMD of sybII ensures rapid transmitter discharge from single vesicles.

Amperometric events are often preceded by a “foot” signal (also referred to as prespike signal), which reflects the trickle of transmitter through a narrow, slowly expanding fusion pore, before its subsequent rapid expansion allows bulk release of neurotransmitter (Chow et al., 1992; Bruns and Jahn, 1995; Albillos et al., 1997). To test whether these distinct phases of transmitter discharge are similarly affected by linker mutations, we re-

stricted our analysis to events preceded by a foot signal. Indeed, insertions of 5, 8, and 14 amino acids gradually prolong the fast phase of transmitter release, indicating that extension of the juxtamembrane region impairs the final, rapid expansion of the fusion pore (Figure S3). In contrast, only a slight reduction in amplitude and prolongation of the prespike signals is observed. Neither the frequency of prespike signals nor their charge is significantly changed. It is possible that dilation of the fusion pore, in its early stage, is largely determined by the dynamics of lipid flow restricted either by areas of high membrane curvature or by a “fence” of hindering transmembrane anchors, as one may suggest from experiments with different v-SNARE TMDs that change the lifetime of the early fusion pore (Borisovska et al., 2005). This scenario would also be compatible with previous findings, showing that synaptotagmin regulates initial fusion pore expansion (Wang et al., 2001), presumably due to stabilization of SNAREs (with their TMDs) around the site of fusion or directly caused by its strong electrostatic interactions with phospholipids (Arac et al., 2006; Bhalla et al., 2006; Zimmerberg et al., 2006). Taken together, linker mutants delay exocytosis initiation and alter final fusion pore enlargement, but appear to leave the intermittent phase of slower pore expansion unchanged.

SybII Mediates Rapid Fluctuations of the Early Fusion Pore

The above findings motivated us to analyze prespike signals more closely. Prespike signals often exhibit rapid fluctuations that clearly exceed the baseline noise (Zhou et al., 1996), but the molecular mechanism underlying these events is not understood. As shown in Figure 5A, fluctuations during the foot signal are short-lived events with durations of less than a millisecond, almost like “subspikes,” and may document the unsuccessful attempt to widen the pore. To study whether v-SNARE proteins affect this fusion pore jitter, we determined the frequency of rapid current changes during the prespike signal by counting suprathreshold deflections of the current derivative (Figure 5A). To identify fluctuations as discrete events

Figure 4. Catecholamine Release from Chromaffin Granules Changes in a Linker Length-Dependent Fashion

(A) Measurements of membrane capacitance (upper panels) and simultaneous amperometric recordings (lower panels) from dko cells expressing sybII (left) or 14 aa linker mutant (right, amino acid insertion: KLGSGSGSGSGS). Dashed line indicates cell opening that initiates intracellular perfusion with high Ca^{2+} -containing solution via the patch pipette.

(B) Pairs of transient oxidation currents with similar charge taken from the recordings in (A) as indicated by the numbering. SybII-events (black) exhibit a faster release time course than 14 aa signals (red) and occasionally saturate the amplifier.

(C) Correlation between mean event frequency and rate of capacitance increase measured for sybII and mutant proteins. Continuous line, linear regression ($r = 0.99$, $p < 0.001$). Frequency data for amperometric events (>4 pA) were determined between 15 and 115 s after cell opening and collected from the following number of cells: sybII (63), 5 aa (11), 8 aa (28), 14 aa (23), 22 aa (24), and dko (11).

(D) Properties of release events (>7 pA) mediated by sybII (black, $n = 6119$), 8 aa mutant (green, $n = 2345$) or 14 aa mutant (red, $n = 1311$), displayed as cumulative frequency distributions for the indicated parameters.

(E) Flash-evoked (exocytotic burst component, Figure 1C) and perfusion-induced capacitance response (ΔC_M , 100 s) as a function of linker length. Data of linker-dependent liposome fusion activity (dashed line) are taken from published results (McNew et al., 1999). Data are normalized to the corresponding sybII response.

(F) Extension of the juxtamembrane region (5 aa, 8 aa, and 14 aa) gradually reduces event amplitude and prolongs transmitter discharge without affecting quantal size. No changes occur with insertion of two proline residues (PP). Values are given as mean for peak amplitude and as median for charge, 50%–90% rise time and half width determined from the parameter's frequency distribution for each cell. Data were averaged from cells with >40 events: sybII (59), 5 aa (11), 8 aa (25), 14 aa (17), PP (14). ** $p < 0.01$, *** $p < 0.001$, one-way analysis of variance versus sybII.

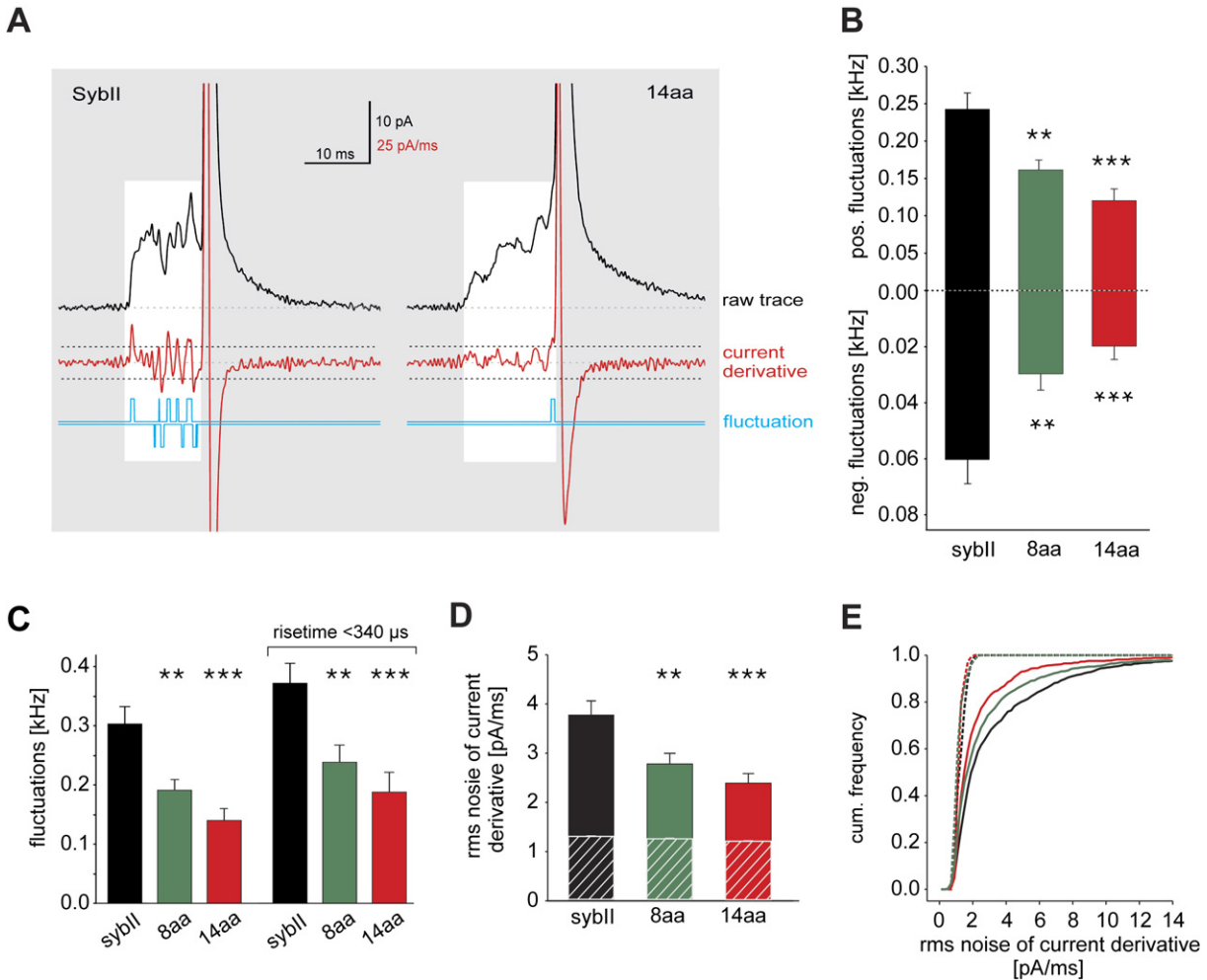


Figure 5. Linker Mutations Diminish Fluctuations of the Early Fusion Pore

(A) Exemplary analysis of current fluctuations during the prespike phase (highlighted area) of transmitter discharge from a chromaffin granule. In the current derivative (red trace), positive and negative excursions beyond the threshold (dashed lines = ± 4 SD of baseline noise) were counted as fluctuations shown in the lower trace (blue). Fluctuations occur more frequently in sybII- (left) than in 14 aa-mediated events (right). The displayed current transients exhibit a similar total charge and 50%–90% rise time (sybII: 445 fC, 320 μ s; 14 aa: 470 fC, 280 μ s) showing that the different fluctuation behavior is not due to differences in diffusional smearing.

(B) Mean frequency of positive and of negative fluctuations decreases with increasing linker length. Data were averaged from dko cells expressing sybII ($n = 23$), 8 aa mutant ($n = 20$) and 14 aa mutant ($n = 16$). Note the different scaling for positive and negative fluctuations.

(C) The average fluctuation frequency (sum of positive and negative fluctuations) of all events with an amplitude > 7 pA as well as of events with spike rise times < 340 μ s decreases in a linker-length dependent fashion.

(D) Mean rms noise of the current derivative during the prespike signal. Hatched bars give values of corresponding background noise. Note that the rms value of the current derivative is a threshold-independent parameter of current noise and is resistant to differences in the average slope among prespike signals.

(E) Cumulative frequency distribution of rms noise for prespike signals (continuous lines) and baseline segments (dashed lines). Data were collected from cells/prespike signals measured for sybII (black) 23/1541, 8 aa (green) 20/1016 and 14 aa (red) 16/768. ** $p < 0.01$, *** $p < 0.001$, one-way analysis of variance versus sybII.

during the prespike with reasonable fidelity, foot signals with a minimum duration of 2 ms were analyzed. Both positive and negative going deflections were detected. Their frequencies are strongly diminished by extending the length of the juxtamembrane region (Figure 5B). On average, the fluctuation frequency is significantly reduced from 300 ± 30 Hz for sybII-mediated events to 190 ± 18 Hz for the 8 aa mutant and even further attenuated

for the 14 aa mutant (140 ± 20 Hz, Figure 5C). An alternative source of rapid current changes in the record might be randomly occurring noise fluctuations. The “false” event rate (λ_f), based on random noise, is given by $\lambda_f = f_c e^{-\theta^2/2rms^2}$ (Colquhoun and Sigworth, 1995). For nearly identical baseline noise (rms) of about 1.34 pA/ms in sybII and mutant recordings (Figure 5D, hatched bars), a threshold (θ) of 6 pA/ms and an effective bandwidth (f_c) of

1.2 kHz, the “false” event rate is 0.05 Hz representing less than one thousandth of the observed fluctuation frequencies. Moreover, a similar phenotype is observed when we selected amperometric spikes with fast rise times (<340 μ s), showing that properties of the release process rather than experimental inconsistencies like diffusional broadening are responsible for the observed differences in fluctuation frequency (Figure 5C). As shown in Figure 5A, current changes during the prespike signal of the 14 aa mutant often remain subthreshold due to their slower kinetics. To corroborate our observations, we also determined the root-mean-square (rms) noise of the current derivative during the prespike signal, serving as a threshold independent parameter for fusion pore jitter. In good agreement with our fluctuation analysis, the 8 aa and the 14 aa insertion strongly diminishes rms noise of prespike signals (Figure 5D). The frequency distributions of rms values illustrate higher current noise during the prespike signal (Figure 5E, continuous lines) compared with baseline noise (dotted lines). Furthermore, they demonstrate the graded reduction of rms values for 8 aa and 14 aa signals (Figure 5E). Taken together, v-SNARE action directly controls fluctuations of the initial fusion pore. It is likely that “linkers,” as flexible intermittent elements between the SNARE domain and the TMD, attenuate high frequency oscillations of the molecular machinery, illustrating the attempt of the SNARE engine to widen the pore.

DISCUSSION

The assembly of SNARE complexes is thought to bring vesicle and plasma membrane into close apposition and to mediate membrane fusion. This hypothesis is largely based on *in vitro* evidence, showing on one hand that synaptobrevin and syntaxin bind with their membrane-proximal parts in a parallel fashion (Hanson et al., 1997; Lin and Scheller, 1997), and on the other hand that SNARE proteins can induce fusion between synthetic liposomes (Weber et al., 1998; Nickel et al., 1999; Pobbati et al., 2006). When and how SNAREs work *in vivo* is still under debate. In particular, evidence for hallmarks of the SNARE hypothesis, that these proteins provide the molecular force for fusion of secretory organelles and act at the moment of intracellular Ca^{2+} increase has not been presented. Our experiments show how key properties of the exocytotic mechanism gradually change by increasing the intramolecular distance between SNARE domain and TMD and provide the first evidence for millisecond action of SNAREs in mediating Ca^{2+} -triggered membrane fusion. Using a combination of high-resolution techniques, we track v-SNARE function from pre- to postfusional stages of exocytosis and delineate a continuous line of v-SNARE actions from priming to complete membrane merger (Figure 6).

According to the hypothesis of N- to C-terminal “zippering” of SNAREs during exocytosis, priming of vesicles is assumed to coincide with initial N-terminal SNARE complex assembly (Hua and Charlton, 1999; Borisovska et al.,

2005; Sorensen et al., 2006). Interestingly, linker mutations gradually reduce the burst component of granule exocytosis, showing that length and/or flexibility of the juxtamembrane region, at the C-terminal end of sybII’s cytoplasmic domain, are critical for granule priming. Given this observation, one might speculate that linker-mediated attenuation of the exocytotic burst simply reflects inefficient targeting of the mutant protein to chromaffin granules or its inability to assemble with SNARE partners in an unperturbed fashion. Several lines of evidence render these possibilities unlikely. First, immunofluorescence analyses reveal no differences in the level or pattern of protein expression between sybII and its mutants. Second, overexpression of the 22 aa mutant in wild-type cells strongly suppresses exocytosis, providing functional evidence for correct protein targeting and suggesting that even such long linker mutants are able to interact with their cognate SNARE partners. Furthermore, exocytotic activity in response to a long-lasting calcium stimulus, as measured in our perfusion experiments, is nearly unaffected by the 8 aa insertion, which abolishes the exocytotic burst. This indicates a particularly stringent length requirement of the juxtamembrane region for granule priming and contrasts a general interference with SNARE complex assembly. In the context of trans-SNARE complexes, our results rather emphasize the importance of a short distance between vesicle and plasma membrane for establishment or maintenance of the release-ready state. Since an insertion of 8 amino acids suffices to eliminate the exocytotic burst, an increase in intermembrane distance of ~ 2 –3 nm appears to be critical. This compares well with dimensions of an intermembranous stalk in which the two contacting monolayers become continuous via an hour-glass-shaped membrane structure (Yang and Huang, 2002; Chernomordik and Kozlov, 2005), making it possible that primed vesicles are not only closely associated with the plasma membrane, but are hemifused organelles held in place by molecular straining of SNARE complexes and awaiting the calcium stimulus. Together with synaptotagmin’s ability to buckle membranes of liposomes (Martens et al., 2007), it is conceivable that close arrangement of SNAREs and synaptotagmin around the fusion site stabilizes secretory organelles in the hemifused state. Such a scenario would also agree with recent studies, showing that cortical granules of the sea urchin are hemifused with the plasma membrane prior to fertilization (Wong et al., 2007). Regardless of the exact underlying mechanism, our results demonstrate that even early stages of exocytosis, such as priming, demand a remarkably tight molecular link between the SNARE motif and the transmembrane anchor of sybII.

Timing of Ca^{2+} -triggered secretion is considered to be controlled by synaptotagmin (Chapman, 2002). Disruption of the synaptotagmin I gene abolishes synchronized transmitter release (Geppert et al., 1994) and Ca^{2+} -binding mutants change the secretory delay as well as the apparent Ca^{2+} sensitivity of secretion (Fernandez-Chacon et al., 2001; Sorensen et al., 2003). In the same line, mutations in

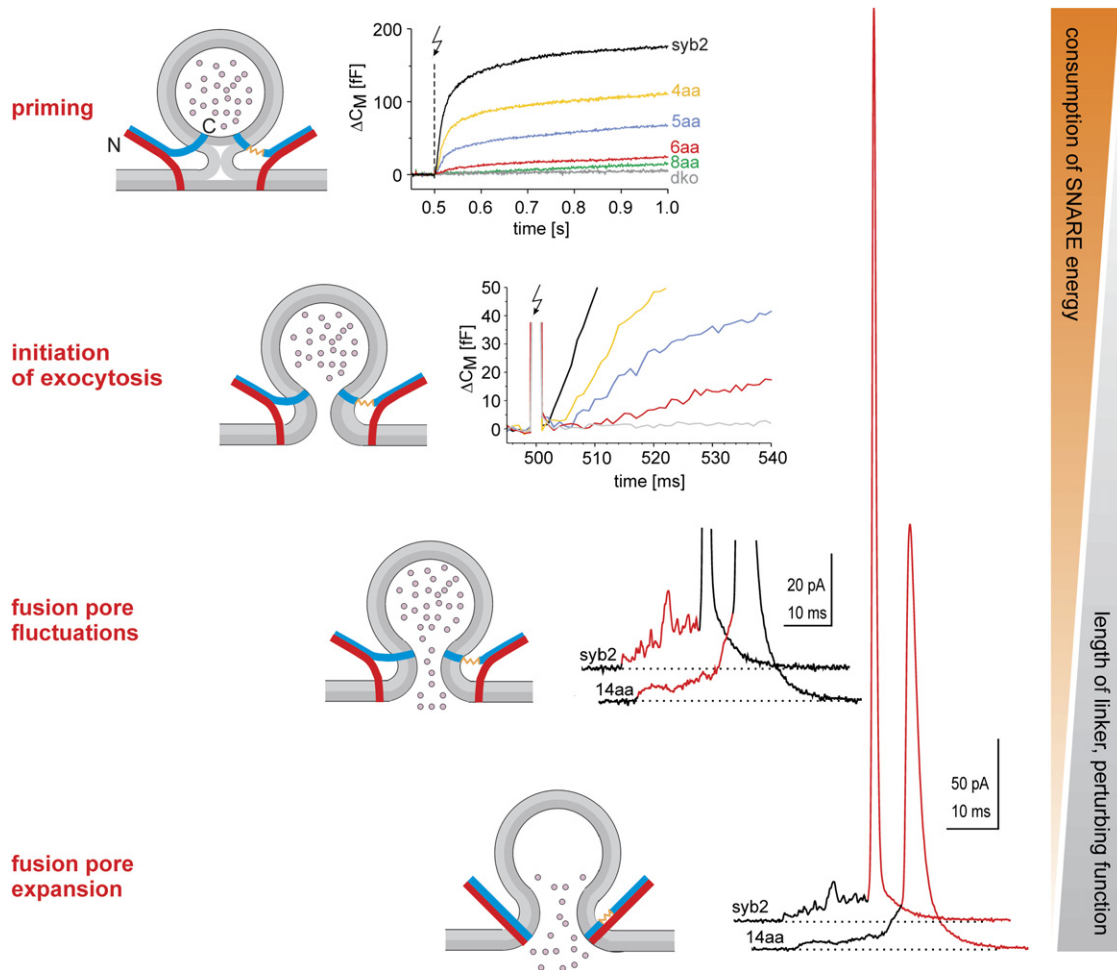


Figure 6. Hypothetical Model of SNARE Action throughout Exocytosis

The combined data set illustrates multiple v-SNARE actions from priming to complete membrane merger. Note that the length of the linker, which suffices to perturb function, increases from early to late stages of exocytosis. This may parallel the progressive conversion of *trans*-SNARE complexes to their *cis*-orientation reflecting high and low energy states of the fusion machinery, respectively.

the C-terminal end of the SNARE complex or truncated versions of SNAP-25 affect exocytosis triggering and also the Ca^{2+} sensitivity of secretion, which may indicate defective synaptotagmin binding to the SNARE complex (Sakaba et al., 2005; Sorensen et al., 2006). Recent experiments with sybII-deficient neurons have shown that long insertions of 12 or 24 amino acids between the SNARE motif and the TMD interfere with synaptobrevin's ability to mediate Ca^{2+} -evoked exocytosis (Deak et al., 2006). Yet, even the shortest mutation used in this study is too long to restore efficient synchronized exocytosis, precluding the observation of linker length-dependent changes in Ca^{2+} -triggered secretion. Our results show that extending the length of the v-SNARE's juxtamembrane region gradually delays the onset of exocytosis, without affecting its Ca^{2+} sensitivity. Linker mutants neither alter the Ca^{2+} -dependent rates of capacitance increase (rate of RRP and SRP) nor the Ca^{2+} threshold for secretion indicating a syn-

aptotagmin-independent change in exocytosis timing. Since synaptotagmin I binds to the carboxy-terminal end of the SNARE complex (Zhang et al., 2002; Dai et al., 2007), about 10–20 amino acids upstream of the site of insertions, it is unlikely that linker mutations destabilize the membrane-proximal part of the SNARE complex or change its overall conformation that should affect binding of synaptotagmin and the Ca^{2+} sensitivity of secretion. Thus, the linker phenotype highlights a postcalcium action of v-SNAREs in stimulus-secretion coupling and suggests that SNAREs are the proteins that exert force on membranes to initiate fusion. Taken together, these results indicate that v-SNAREs drive Ca^{2+} -triggered membrane fusion at the millisecond time scale.

Mechanisms that control fusion pore expansion determine the rate of transmitter release from the fusing organelle and thus strength and fidelity of chemical signaling between cells. Previous studies on norepinephrine release

from PC12 cells suggested that mutations within the hydrophobic layers throughout the SNARE complex change the lifetime of the early fusion pore, albeit without any preference for C- or N-terminal location within the SNARE motif (Han and Jackson, 2006). This finding has been interpreted as evidence against vectorial “zipping” of SNAREs and led to the suggestion that partial disassembly of the SNARE complex governs initial fusion pore expansion. Our results are difficult to reconcile with such a scenario. First, they show that linker extensions attenuate fluctuations of the early fusion pore, suggesting that molecular tension on the TMD of sybll persists even after initiation of exocytosis. Second, they slow down the fast phase of transmitter discharge from granules, indicating that v-SNARE action is continued throughout the final, rapid expansion of the pore. Thus, SNARE proteins not only provide sufficient energy to initiate exocytosis, but also to accelerate merger of membranes. In contrast to the clear changes in the properties of the amperometric spike, we failed to observe similarly significant alterations for the lifetime of the early fusion pore. Considering the kinetic differences between prespike (slow) and spike phase (fast), it seems likely that distinct mechanisms govern their overall time courses. An attractive explanation could be that interactions of synaptotagmin with t-SNARE proteins, hinder early fusion pore expansion, as has been suggested by experiments in PC12 cells (Wang et al., 2001; Bai et al., 2004). With progressive pore widening these interactions are diminished, enabling an unhindered pull of SNAREs on their TMDs to complete membrane merger. Overall, our observations support a picture wherein mechanical coupling between v- and t-SNARE proteins motorizes exocytosis throughout its different stages. Therefore, it seems likely that continuous molecular straining by SNARE proteins together with synaptotagmin’s ability to control SNAREs and phospholipids guide the vesicle on the way toward complete fusion.

Based on these results, it stands to reason that short linkers should dissipate force generated by SNARE assembly less effectively than long linkers. In comparison with the wild-type protein, short insertions like the 5 aa mutant, have a greater impact on priming (>2-fold reduction) and stimulus-secretion coupling (2-fold increase) than on later stages of exocytosis, such as fusion pore enlargement (12% increase in 50%–90% rise time). Long insertions (e.g., 14 aa), on the other hand, efficiently perturb the latter process, pointing to its lower energy state. Thus, the differential attenuation of early and late stages of exocytosis by short and long linkers draws a downhill-oriented energy landscape that may reflect the progressive conversion of energy-providing SNARE complexes from their *trans*- to the *cis*-orientation (low energy, all proteins in the same membrane). Although synchronous and asynchronous exocytosis absolutely depend on the function of v-SNAREs, as demonstrated by their nearly complete block in dko cells, they strongly differ regarding their sensitivity to extensions of the v-SNARE’s juxtamembrane region (Figure 4E). This suggests that synchronous exocytosis

demands more force from the SNARE machinery than asynchronous exocytosis. The resistance of asynchronous exocytosis to short extensions fits well with that of liposome fusion activity solely promoted by heterotrimeric SNARE complexes (Figure 4E). Perhaps other proteins like complexin, which are needed for rapid stimulus-secretion coupling and arrest fusion of liposomes at hemifusion (Reim et al., 2001; Giraudo et al., 2006; Schaub et al., 2006; Tang et al., 2006), produce extra energy costs paid by the SNARE engine as a tribute for synchronization.

In summary, our observations pinpoint the function of v-SNARE proteins throughout different stages of exocytosis and provide *in vivo* evidence for the role of SNAREs in executing Ca²⁺-triggered membrane fusion. Yet, elucidating the function of SNARE proteins in the context of their supramolecular organization together with other scaffolding proteins is required for a true understanding of the mechanisms of transmitter release.

EXPERIMENTAL PROCEDURES

Mutant Mice and Cell Culture

Experiments were performed with embryonic chromaffin cells that were prepared at E17.5–E18.5 from double-v-SNARE knockout mice and cultured as described (Borisovska et al., 2005). Recordings were done at room temperature on days 1–3 in culture and 6–7 hr after infection of cells with virus particles.

Viral Constructs

cDNAs encoding for sybll and its mutants were subcloned into the viral plasmid pSFV1 (Invitrogen) upstream of an independent open reading frame that encodes for enhanced green fluorescent protein (EGFP). EGFP labeling was used to identify infected cells. Mutant constructs carrying either amino acid insertions of different length or a double-proline insertion at amino acid position 94 were generated using the overlapping primer method as described (Higuchi, 1989). Note that substitution of lysine residues (K91A and K94A) with alanine residues causes missorting of the expressed sybll variant, similar to that observed with the truncated TMD shown in Figure S2. Therefore, we kept the membrane proximal lysine residue (aa 94) downstream as well as the KNLK motif upstream of the insertion. This was best accomplished by generating two KL sites, which encode for HindIII restriction sites and allow in turn for a primer-based elongation of the inserted amino acid stretch to facilitate the cloning process as described previously (McNew et al., 1999). All mutations were confirmed by DNA sequence analysis. Virus particles were produced as described (Ashery et al., 1999).

Whole-Cell Capacitance Measurements and Amperometry

Whole-cell membrane capacitance measurements and photolysis of caged Ca²⁺ as well as ratiometric measurements of [Ca²⁺]_i were performed as described (Borisovska et al., 2005). The extracellular Ringer’s solution contained (in mM): 130 NaCl, 4 KCl, 2 CaCl₂, 1 MgCl₂, 10 HEPES, 30 Glucose, pH 7.3 with NaOH. The pipette solution for flash experiments contained (in mM): 110 Cs-Glutamate, 8 NaCl, 3.5 CaCl₂, 5 NP-EGTA, 0.2 Fura-2, 0.3 Fura-2, 2 MgATP, 0.3 Na₂GTP, 40 HEPES, (pH 7.3), 320 mOsm. For Ca²⁺-ramp experiments, cells were perfused with the same solution, but with 50% Ca²⁺-loaded NP-EGTA (7.5 NP-EGTA and 3.5 Ca²⁺) to lower the resting level of [Ca²⁺]_i, before starting the ramp protocol. The flash-evoked capacitance response was approximated with the following function: $f(x) = A_0 + A_1 (1 - \exp[-t/\tau_1]) + A_2 (1 - \exp[-t/\tau_2]) + kt$ where A₀ represents the cell capacitance before the flash. The parameters A₁, τ₁, and A₂, τ₂ represent the amplitudes and time constants of RRP

and SRP, respectively. The exocytotic delay is defined as the time between the flash and the intersection point of the back-extrapolated fast exponential with the baseline (Figure 2B). For Ca^{2+} infusion experiments, the pipette solution contained (in mM): 110 Cs-Glutamate, 8 NaCl, 20 DPTA, 5 CaCl_2 , 0.2 Fura-2, 0.3 Fura-2, 2 MgATP, 0.3 Na_2GTP , 40 HEPES, pH 7.3, 19 μM free calcium. Amperometric recordings with an EPC7 amplifier (HEKA Electronic, Inc.) and carbon fiber electrodes (5 μm diameter, Amoco) were performed as previously described (Bruns, 2004). Current signals were filtered at 2 kHz and digitized gap-free at 25 kHz. Amperometric spikes with a charge ranging from 10–5000 fC and peak amplitude > 4 pA were selected for frequency analysis, while an amplitude criterion of > 7 pA was set for the analysis of single spike characteristics. The start of the foot signal is defined as the time point where the current amplitude exceeds two times the standard deviation of the average baseline noise and it ends at the inflection point (determined from maximum of the current second derivative) between the slowly increasing foot signal and the rapidly increasing spike current. For foot flicker analysis, the current derivative was again filtered at 1.2 kHz and fluctuations exceeding the threshold of ± 6 pA/ms (~ 4 times SD of baseline noise) were counted. The number of suprathreshold fluctuations divided by the corresponding foot duration defines the fluctuation frequency. Values are given at mean \pm s.e.m. if not indicated otherwise.

Immunocytochemistry

Chromaffin cells were processed 6 hr after virus infection for immunolabeling as described (Hannah et al., 1998). Epifluorescence pictures were acquired with an AxioCam MRm-CCD camera (Carl Zeiss, Inc.) and analyzed with Metamorph software (Universal Imaging Inc.). The mouse monoclonal antibody against syb11 (69.1, antigen epitope amino acid position 1–14) was kindly provided by R. Jahn (Göttingen, Germany). For quantification, the average intensity of the fluorescent immunolabel was determined within an area of interest comprising the outer cell perimeter.

Author Contribution

Maria Borisovska and Jaideep Kesavan have contributed equally to this work.

Supplemental Data

Supplemental Data include three figures and Supplemental References and can be found with this article online at <http://www.cell.com/cgi/content/full/131/2/351/DC1>.

ACKNOWLEDGMENTS

The authors are grateful to Drs. J. Rettig, F. Zufall, T. Leinders-Zufall, and D. Stevens for valuable discussions, and to Y. Schwarz for help with viral infection of chromaffin cells. We thank K. Klingler, K. Schmidt, T. Mayer, and M. Wirth for excellent technical assistance. The work was supported by grants from the Deutsche Forschungsgemeinschaft (DFG) (SFB 530 and GRK1326) to D.B. and by HOMFOR.

Received: July 3, 2007

Revised: August 28, 2007

Accepted: September 17, 2007

Published: October 18, 2007

REFERENCES

Albillos, A., Dernick, G., Horstmann, H., Almers, W., Alvarez de Toledo, G., and Lindau, M. (1997). The exocytotic event in chromaffin cells revealed by patch amperometry. *Nature* 389, 509–512.

Arac, D., Chen, X., Khant, H.A., Ubach, J., Ludtke, S.J., Kikkawa, M., Johnson, A.E., Chiu, W., Sudhof, T.C., and Rizo, J. (2006). Close membrane-membrane proximity induced by Ca^{2+} -dependent multivalent

binding of synaptotagmin-1 to phospholipids. *Nat. Struct. Mol. Biol.* 13, 209–217.

Ashery, U., Betz, A., Xu, T., Brose, N., and Rettig, J. (1999). An efficient method for infection of adrenal chromaffin cells using the Semliki Forest virus gene expression system. *Eur. J. Cell Biol.* 78, 525–532.

Bai, J., Wang, C.T., Richards, D.A., Jackson, M.B., and Chapman, E.R. (2004). Fusion pore dynamics are regulated by synaptotagmin¹ t-SNARE interactions. *Neuron* 41, 929–942.

Bhalla, A., Chicka, M.C., Tucker, W.C., and Chapman, E.R. (2006). Ca^{2+} -synaptotagmin directly regulates t-SNARE function during reconstituted membrane fusion. *Nat. Struct. Mol. Biol.* 13, 323–330.

Borisovska, M., Zhao, Y., Tsytsyura, Y., Glyvuk, N., Takamori, S., Matti, U., Rettig, J., Sudhof, T., and Bruns, D. (2005). v-SNAREs control exocytosis of vesicles from priming to fusion. *EMBO J.* 24, 2114–2126.

Bowen, M.E., Weninger, K., Brunger, A.T., and Chu, S. (2004). Single molecule observation of liposome-bilayer fusion thermally induced by soluble N-ethyl maleimide sensitive-factor attachment protein receptors (SNAREs). *Biophys. J.* 87, 3569–3584.

Bruns, D. (2004). Detection of transmitter release with carbon fiber electrodes. *Methods* 33, 312–321.

Bruns, D., and Jahn, R. (1995). Real-time measurement of transmitter release from single synaptic vesicles. *Nature* 377, 62–65.

Chapman, E.R. (2002). Synaptotagmin: a Ca^{2+} sensor that triggers exocytosis? *Nat. Rev. Mol. Cell Biol.* 3, 498–508.

Chernomordik, L.V., and Kozlov, M.M. (2005). Membrane hemifusion: crossing a chasm in two leaps. *Cell* 123, 375–382.

Chow, R.H., von Ruden, L., and Neher, E. (1992). Delay in vesicle fusion revealed by electrochemical monitoring of single secretory events in adrenal chromaffin cells. *Nature* 356, 60–63.

Colquhoun, D., and Sigworth, F.J. (1995). Fitting and Statistical analysis of Single-Channel Records. In *Single-Channel Recording*, B. Sakmann and E. Neher, eds. (New York: Plenum Press), pp. 483–585.

Dai, H., Shen, N., Arac, D., and Rizo, J. (2007). A quaternary SNARE-synaptotagmin- Ca^{2+} -phospholipid complex in neurotransmitter release. *J. Mol. Biol.* 367, 848–863.

Deak, F., Shin, O.H., Kavalali, E.T., and Sudhof, T.C. (2006). Structural determinants of synaptobrevin 2 function in synaptic vesicle fusion. *J. Neurosci.* 26, 6668–6676.

Dennison, S.M., Bowen, M.E., Brunger, A.T., and Lentz, B.R. (2006). Neuronal SNAREs do not trigger fusion between synthetic membranes but do promote PEG-mediated membrane fusion. *Biophys. J.* 90, 1661–1675.

Fernandez-Chacon, R., Konigstorfer, A., Gerber, S.H., Garcia, J., Matos, M.F., Stevens, C.F., Brose, N., Rizo, J., Rosenmund, C., and Sudhof, T.C. (2001). Synaptotagmin I functions as a calcium regulator of release probability. *Nature* 410, 41–49.

Geppert, M., Goda, Y., Hammer, R.E., Li, C., Rosahl, T.W., Stevens, C.F., and Sudhof, T.C. (1994). Synaptotagmin I: a major Ca^{2+} sensor for transmitter release at a central synapse. *Cell* 79, 717–727.

Giraud, C.G., Eng, W.S., Melia, T.J., and Rothman, J.E. (2006). A clamping mechanism involved in SNARE-dependent exocytosis. *Science* 313, 676–680.

Giraud, C.G., Hu, C., You, D., Slovic, A.M., Mosharov, E.V., Sulzer, D., Melia, T.J., and Rothman, J.E. (2005). SNAREs can promote complete fusion and hemifusion as alternative outcomes. *J. Cell Biol.* 170, 249–260.

Han, X., and Jackson, M.B. (2006). Structural transitions in the synaptic SNARE complex during Ca^{2+} -triggered exocytosis. *J. Cell Biol.* 172, 281–293.

- Hannah, M.J., Weiss, U., and Huttner, W.B. (1998). Differential extraction of proteins from paraformaldehyde-fixed cells: lessons from synaptophysin and other membrane proteins. *Methods* 16, 170–181.
- Hanson, P.I., Roth, R., Morisaki, H., Jahn, R., and Heuser, J.E. (1997). Structure and conformational changes in NSF and its membrane receptor complexes visualized by quick-freeze/deep-etch electron microscopy. *Cell* 90, 523–535.
- Higuchi, R. (1989). *Using PCR to Engineer DNA* (New York, NY: Stockton Press).
- Hua, S.Y., and Charlton, M.P. (1999). Activity-dependent changes in partial VAMP complexes during neurotransmitter release. *Nat. Neurosci.* 2, 1078–1083.
- Jackson, M.B., and Chapman, E.R. (2006). Fusion pores and fusion machines in Ca²⁺-triggered exocytosis. *Annu. Rev. Biophys. Biomol. Struct.* 35, 135–160.
- Jahn, R., and Scheller, R.H. (2006). SNAREs—engines for membrane fusion. *Nat. Rev. Mol. Cell Biol.* 7, 631–643.
- Lin, R.C., and Scheller, R.H. (1997). Structural organization of the synaptic exocytosis core complex. *Neuron* 19, 1087–1094.
- Martens, S., Kozlov, M.M., and McMahon, H.T. (2007). How synaptotagmin promotes membrane fusion. *Science* 316, 1205–1208.
- McNew, J.A., Weber, T., Engelman, D.M., Sollner, T.H., and Rothman, J.E. (1999). The length of the flexible SNAREpin juxtamembrane region is a critical determinant of SNARE-dependent fusion. *Mol. Cell* 4, 415–421.
- Nagy, G., Kim, J.H., Pang, Z.P., Matti, U., Rettig, J., Sudhof, T.C., and Sorensen, J.B. (2006). Different effects on fast exocytosis induced by synaptotagmin 1 and 2 isoforms and abundance but not by phosphorylation. *J. Neurosci.* 26, 632–643.
- Nickel, W., Weber, T., McNew, J.A., Parlati, F., Sollner, T.H., and Rothman, J.E. (1999). Content mixing and membrane integrity during membrane fusion driven by pairing of isolated v-SNAREs and t-SNAREs. *Proc. Natl. Acad. Sci. USA* 96, 12571–12576.
- Pobbati, A.V., Stein, A., and Fasshauer, D. (2006). N- to C-terminal SNARE complex assembly promotes rapid membrane fusion. *Science* 313, 673–676.
- Reese, C., Heise, F., and Mayer, A. (2005). Trans-SNARE pairing can precede a hemifusion intermediate in intracellular membrane fusion. *Nature* 436, 410–414.
- Reim, K., Mansour, M., Varoqueaux, F., McMahon, H.T., Sudhof, T.C., Brose, N., and Rosenmund, C. (2001). Complexins regulate a late step in Ca²⁺-dependent neurotransmitter release. *Cell* 104, 71–81.
- Rettig, J., and Neher, E. (2002). Emerging roles of presynaptic proteins in Ca⁺⁺-triggered exocytosis. *Science* 298, 781–785.
- Sakaba, T., Stein, A., Jahn, R., and Neher, E. (2005). Distinct kinetic changes in neurotransmitter release after SNARE protein cleavage. *Science* 309, 491–494.
- Schaub, J.R., Lu, X., Doneske, B., Shin, Y.K., and McNew, J.A. (2006). Hemifusion arrest by complexin is relieved by Ca²⁺-synaptotagmin I. *Nat. Struct. Mol. Biol.* 13, 748–750.
- Sorensen, J.B., Fernandez-Chacon, R., Sudhof, T.C., and Neher, E. (2003). Examining synaptotagmin 1 function in dense core vesicle exocytosis under direct control of Ca²⁺. *J. Gen. Physiol.* 122, 265–276.
- Sorensen, J.B., Matti, U., Wei, S.H., Nehring, R.B., Voets, T., Ashery, U., Binz, T., Neher, E., and Rettig, J. (2002). The SNARE protein SNAP-25 is linked to fast calcium triggering of exocytosis. *Proc. Natl. Acad. Sci. USA* 99, 1627–1632.
- Sorensen, J.B., Wiederhold, K., Muller, E.M., Milosevic, I., Nagy, G., de Groot, B.L., Grubmuller, H., and Fasshauer, D. (2006). Sequential N- to C-terminal SNARE complex assembly drives priming and fusion of secretory vesicles. *EMBO J.* 25, 955–966.
- Sutton, R.B., Fasshauer, D., Jahn, R., and Brunger, A.T. (1998). Crystal structure of a SNARE complex involved in synaptic exocytosis at 2.4 Å resolution. *Nature* 395, 347–353.
- Tang, J., Maximov, A., Shin, O.H., Dai, H., Rizo, J., and Sudhof, T.C. (2006). A complexin/synaptotagmin 1 switch controls fast synaptic vesicle exocytosis. *Cell* 126, 1175–1187.
- Voets, T., Moser, T., Lund, P.E., Chow, R.H., Geppert, M., Sudhof, T.C., and Neher, E. (2001). Intracellular calcium dependence of large dense-core vesicle exocytosis in the absence of synaptotagmin I. *Proc. Natl. Acad. Sci. USA* 98, 11680–11685.
- Voets, T., Neher, E., and Moser, T. (1999). Mechanisms underlying phasic and sustained secretion in chromaffin cells from mouse adrenal slices. *Neuron* 23, 607–615.
- Wang, C.T., Grishanin, R., Earles, C.A., Chang, P.Y., Martin, T.F., Chapman, E.R., and Jackson, M.B. (2001). Synaptotagmin modulation of fusion pore kinetics in regulated exocytosis of dense-core vesicles. *Science* 294, 1111–1115.
- Weber, T., Zemelman, B.V., McNew, J.A., Westermann, B., Gmachl, M., Parlati, F., Sollner, T.H., and Rothman, J.E. (1998). SNAREpins: minimal machinery for membrane fusion. *Cell* 92, 759–772.
- Wong, J.L., Koppel, D.E., Cowan, A.E., and Wessel, G.M. (2007). Membrane hemifusion is a stable intermediate of exocytosis. *Dev. Cell* 12, 653–659.
- Xu, Y., Zhang, F., Su, Z., McNew, J.A., and Shin, Y.K. (2005). Hemifusion in SNARE-mediated membrane fusion. *Nat. Struct. Mol. Biol.* 12, 417–422.
- Yang, L., and Huang, H.W. (2002). Observation of a membrane fusion intermediate structure. *Science* 297, 1877–1879.
- Zhang, X., Kim-Miller, M.J., Fukuda, M., Kowalchuk, J.A., and Martin, T.F. (2002). Ca²⁺-dependent synaptotagmin binding to SNAP-25 is essential for Ca²⁺-triggered exocytosis. *Neuron* 34, 599–611.
- Zhou, Z., Mislis, S., and Chow, R.H. (1996). Rapid fluctuations in transmitter release from single vesicles in bovine adrenal chromaffin cells. *Biophys. J.* 70, 1543–1552.
- Zimmerberg, J., Akimov, S.A., and Frolov, V. (2006). Synaptotagmin: fusogenic role for calcium sensor? *Nat. Struct. Mol. Biol.* 13, 301–303.